PERGAMON

Annals of Nuclear Energy 27 (2000) 1607–1626

annals of NUCLEAR ENERGY

www.elsevier.com/locate/anucene

Coupled scalar and vector P_N methods for solving multigroup transport problems in multislab geometry

A. F. Dias,[a] R. D. M. Garcia[a,b]

[a] *Centro Técnico Aeroespacial, Instituto de Estudos Avançados, 12231-970 São José dos Campos, SP, Brazil*

[b] *HSH Scientific Computing, Rua Carlos de Campos 286, 12242-540 São José dos Campos, SP, Brazil*

Received 7 April 2000; accepted 14 April 2000

Abstract

A spherical-harmonics (P_N) method that incorporates and couples existent scalar and vector versions of the method is developed. The scalar (group-by-group) version of method is applied to the slowing-down energy range and the vector version to the thermal energy range. The link of coupling between these methods is the slowing-down source to the thermal groups which becomes available once the problems for all of the slowing-down groups are solved with the scalar method. The advantage of using the coupled P_N method over the vector method when solving transport problems defined in extended energy ranges is demonstrated in this work.

1. Introduction

Until the works of Caldeira, Dias and Garcia appeared in the literature (Caldeira et al., 1998a; 1998b), the only available option for developing spatially continuous P_N solutions for multigroup transport problems was (what we call) the vector P_N method, developed and used by various authors along the years (Davison, 1957; Lee et al., 1985; Siewert, 1993a). This version of the method solves a matrix transport equation that allows particle transfer between any two groups in the group structure and gives a solution for all groups at the same time (no iteration over the groups is required). This approach is clearly adequate for neutronics problems defined exclusively in the thermal energy range or problems that involve fission, but, as will be shown in this paper, it is not the best way of implementing the P_N method for solving shielding problems defined in the full range of energies that is of interest for fission technology (typically, 0–20 MeV). A coupling between the scalar P_N method (Caldeira et al., 1998a; 1998b) and the vector P_N method in the formulation of Siewert (1993a) seems to be the best choice for this class of problems.

The outline of this paper is as follows. In Sections 2 and 3 we summarize, respectively, the scalar and the vector P_N methods that embody our coupled method for the case of a single slab and in Section 4 we develop the source term which is the link of coupling between these methods. In Section 5 we describe the extension of the coupled method to multislab geometry and in Section 6 we report numerical results for a few test problems and compare the computational performance of the methods. Finally, Section 7 consists of our concluding remarks.

PII: S0306-4549(00)00046-3

2. The scalar P_N method

We assume that the problem we wish to solve is defined in a group structure with G groups, the first G_d of which belong to the slowing-down range, where only downscattering is present, and the remaining $G_u = G - G_d$ to the thermal range, where upscattering is present in addition to downscattering, except in the highest-energy group.

Thus, in the slowing-down range we consider, for groups $i = 1, 2, \ldots, G_d$, the problem defined by the transport equation, for $z \in (z_L, z_R)$ and $\mu \in [-1, 1]$,

$$\mu \frac{\partial}{\partial z}\psi_i(z,\mu) + \sigma_i \psi_i(z,\mu) = \frac{1}{2}\sum_{j=1}^{i}\sum_{\ell=0}^{\mathcal{L}} \sigma_{ij}(\ell) P_\ell(\mu) \int_{-1}^{1} P_\ell(\mu')\psi_j(z,\mu')\mathrm{d}\mu' \tag{1}$$

and the boundary conditions, for $\mu \in (0, 1]$,

$$\psi_i(z_L, \mu) = L_i(\mu) \tag{2a}$$

and

$$\psi_i(z_R, -\mu) = R_i(\mu), \tag{2b}$$

where the incident particle distributions $L_i(\mu)$ and $R_i(\mu)$ are supposed known. In Eq. (1), $\psi_i(z,\mu)$ is the particle angular flux for group i at position z and direction of particle travel defined by the cosine of the polar angle μ, σ_i is the macroscopic total cross section for group i, and $\sigma_{ij}(\ell)$ is the ℓ'th Legendre moment of the transfer cross section for scattering from group j to group i.

For N odd, a P_N solution that satisfies the first $N+1$ moments of Eq. (1) and the Mark prescription (Davison, 1957; Gelbard, 1968) of the boundary conditions expressed by Eqs. (2a) and (2b) was developed by Caldeira et al. (1998a). This solution can be written as

$$\psi_i(z,\mu) = \frac{1}{2}\sum_{n=0}^{N}(2n+1)\phi_{i,n}(z)P_n(\mu), \tag{3}$$

where the Legendre moment

$$\phi_{i,n}(z) = \int_{-1}^{1} \psi_i(z,\mu)P_n(\mu)\mathrm{d}\mu \tag{4}$$

can be shown to be given by (Caldeira et al., 1998a)

$$\phi_{i,n}(z) = \sum_{j=1}^{i}\sum_{k=1}^{K}\left[A_{j,k}\mathrm{e}^{-\sigma_j(z-z_L)/\xi_{j,k}} + (-1)^n B_{j,k}\mathrm{e}^{-\sigma_j(z_R-z)/\xi_{j,k}}\right] g_n^{ij}(\xi_{j,k}), \tag{5}$$

with $K = (N+1)/2$. In this expression, the so-called P_N eigenvalues $\{\pm\xi_{j,k}\}$ are the K pairs of zeros of the Chandrasekhar polynomial $g_{j,N+1}(\xi)$ and $\{g_n^{ij}(\xi_{j,k})\}$ are the *generalized* Chandrasekhar polynomials introduced by Caldeira et al. (1998a). These polynomials must satisfy the tridiagonal system defined by

$$\left(\frac{\sigma_i\xi}{\sigma_j}\right) h_{i,n} g_n^{ij}(\xi) = (n+1)g_{n+1}^{ij}(\xi) + n g_{n-1}^{ij}(\xi) + \left(\frac{\xi}{\sigma_j}\right)\sum_{\alpha=j}^{i-1}\sigma_{i\alpha}(n) g_n^{\alpha j}(\xi) \tag{6}$$

for $n = 0, 1, \ldots, N$ and the truncation condition $g_{N+1}^{ij}(\xi) = 0$ and reduce to the standard Chandrasekhar polynomials $\{g_{j,n}(\xi_{j,k})\}$ when the source group j is the same as the sink group i. We note that the above formulation is valid on the assumption that $\sigma_i\xi_{j,k} \neq \sigma_j\xi_{i,k'}$ for $k, k' = 1, 2, \ldots, K$, and that the case where one or more of these conditions are not satisfied by a given pair of sink and source groups was resolved by Caldeira et al. (1998b). In addition, we note that $h_{i,n} = 2n + 1 - \sigma_{ii}(n)/\sigma_i$ for $n \leq \mathcal{L}$ and $h_{i,n} = 2n+1$ for $n > \mathcal{L}$.

To complete the P_N solution expressed by Eqs. (3) and (5), we can follow Caldeira et al. (1998a) and use the Mark prescription of the boundary conditions expressed by Eqs. (2a) and (2b), i.e.

$$\psi_i(z_L, \mu_m) = L_i(\mu_m) \tag{7a}$$

and

$$\psi_i(z_R, -\mu_m) = R_i(\mu_m), \tag{7b}$$

where μ_m, $m = 1, 2, \ldots, K$, are the *positive* zeros of $P_{N+1}(\mu)$, along with the definitions $\Delta = z_R - z_L$,

$$X_i(\xi, \mu) = \frac{1}{2}\sum_{n=0}^{N}(2n+1)g_{i,n}(\xi)P_n(\mu), \tag{8a}$$

$$Y_i(\xi, \mu) = \frac{1}{2}\sum_{n=0}^{N}(-1)^n(2n+1)g_{i,n}(\xi)P_n(\mu), \tag{8b}$$

$$X^{ij}(\xi, \mu) = \frac{1}{2}\sum_{n=0}^{N}(2n+1)g_n^{ij}(\xi)P_n(\mu) \tag{8c}$$

and

$$Y^{ij}(\xi, \mu) = \frac{1}{2}\sum_{n=0}^{N}(-1)^n(2n+1)g_n^{ij}(\xi)P_n(\mu), \tag{8d}$$

to deduce the linear system of algebraic equations

$$\sum_{k=1}^{K}\left[A_{i,k}X_i(\xi_{i,k;}\,\mu_m) + B_{i,k}Y_i(\xi_{i,k}, \mu_m)\mathrm{e}^{-\sigma_i\Delta/\xi_{i,k}}\right] = L_i(\mu_m) - \sum_{j=1}^{i-1}\sum_{k=1}^{K}\left[A_{j,k}X^{ij}(\xi_{j,k}, \mu_m) + B_{j,k}Y^{ij}(\xi_{j,k}, \mu_m)\mathrm{e}^{-\sigma_j\Delta/\xi_{j,k}}\right] \tag{9a}$$

and

$$\sum_{k=1}^{K}\left[B_{i,k}X_i(\xi_{i,k}, \mu_m) + A_{i,k}Y_i(\xi_{i,k}, \mu_m)\mathrm{e}^{-\sigma_i\Delta/\xi_{i,k}}\right] = R_i(\mu_m) - \sum_{j=1}^{i-1}\sum_{k=1}^{K}\left[B_{j,k}X^{ij}(\xi_{j,k}, \mu_m) + A_{j,k}Y^{ij}(\xi_{j,k}, \mu_m)\mathrm{e}^{-\sigma_j\Delta/\xi_{j,k}}\right], \tag{9b}$$

$m = 1, 2, \ldots, K$, for the unknown coefficients $\{A_{i,k}\}$ and $\{B_{i,k}\}$ of group i. Assuming that the solutions for groups $1, 2, \ldots, i-1$ have been found in previous applications of the method, the right-hand sides of Eqs. (9a) and (9b) are known, and so, once the linear system defined by these equations is solved, we have at hand all quantities needed to evaluate the P_N solution to Eqs. (1) and (2). We note that the scalar fluxes and currents in group i are simply the first two Legendre moments $\phi_{i,0}(z)$ and $\phi_{i,1}(z)$ obtained by setting $n = 0$ and $n = 1$ in Eq. (5) and can be accurately computed using that equation. The same is true in regard to the partial currents

$$J_i^{\pm}(z) = \int_0^1 \mu\psi_i(z, \pm\mu)\mathrm{d}\mu, \tag{10}$$

which can be expressed (Garcia and Siewert, 1996) in terms of the Legendre moments $\phi_{i,0}(z)$, $\phi_{i,1}(z)$ and $\phi_{i,n}(z)$, $n = 2, 4, 6, \ldots, N-1$. Finally, to compute the angular flux $\psi_i(z, \mu)$, Caldeira et al. (1998a) have used the source-function integration technique (Kourganoff, 1952; Dave and Armstrong, 1974; Karp, 1981; Siewert, 1993b; Garcia, 2000) to derive postprocessed formulas [see their Eqs. (21) and (23)] that effectively smooth out the oscillations observed when one tries to use Eqs. (3) and (5) for computing the angular flux.

3. The vector P_N method

In regard to the thermal groups $i = G_d+1, G_d+2, \ldots, G$, since they can all be coupled by particle transfer we prefer to deal with the matrix transport equation (Siewert, 1993a), for $z \in (z_L, z_R)$ and $\mu \in [-1, 1]$,

$$\mu \frac{\partial}{\partial z}\mathbf{\Psi}(z,\mu) + \mathbf{\Sigma}\mathbf{\Psi}(z,\mu) = \frac{1}{2}\sum_{\ell=0}^{\mathcal{L}} P_\ell(\mu)\mathbf{C}_\ell \int_{-1}^{1} P_\ell(\mu')\mathbf{\Psi}(z,\mu')\mathrm{d}\mu' + \mathbf{Q}(z,\mu), \tag{11}$$

where

$$\mathbf{\Psi}(z,\mu) = \begin{pmatrix} \psi_{G_d+1}(z,\mu) \\ \psi_{G_d+2}(z,\mu) \\ \vdots \\ \psi_G(z,\mu) \end{pmatrix} \tag{12}$$

is a vector of dimension $G_u = G - G_d$ with the desired thermal angular fluxes as components, $\mathbf{\Sigma}$ is a diagonal matrix of order G_u with the macroscopic total cross sections σ_i, $i = G_d+1, G_d+2, \ldots, G$, as diagonal elements,

$$\mathbf{C}_\ell = \begin{pmatrix} \sigma_{G_d+1,G_d+1}(\ell) & \sigma_{G_d+1,G_d+2}(\ell) & \cdots & \sigma_{G_d+1,G}(\ell) \\ \sigma_{G_d+2,G_d+1}(\ell) & \sigma_{G_d+2,G_d+2}(\ell) & \cdots & \sigma_{G_d+2,G}(\ell) \\ \vdots & \vdots & \ddots & \vdots \\ \sigma_{G,G_d+1}(\ell) & \sigma_{G,G_d+2}(\ell) & \cdots & \sigma_{G,G}(\ell) \end{pmatrix} \tag{13}$$

is a $G_u \times G_u$ matrix with the ℓ'th Legendre moments of the transfer cross sections as elements, and

$$\mathbf{Q}(z,\mu) = \begin{pmatrix} Q_{G_d+1}(z,\mu) \\ Q_{G_d+2}(z,\mu) \\ \vdots \\ Q_G(z,\mu) \end{pmatrix} \tag{14}$$

is a vector of dimension G_u with the downscatter sources to the thermal groups as components. Here, to simplify our presentation, we prefer to keep the downscatter sources $\{Q_i(z,\mu)\}$ as yet unspecified; explicit expressions for these sources and related quantities will be given in the next section. In this section we only use the fact that, since the downscatter sources are directly related to the angular fluxes in the slowing-down range and we have used in Section 2 a P_N approximation to represent these fluxes, only the first $N+1$ Legendre moments of these sources can be $\neq 0$.

At this point, we note that our formulation differs slightly from that of Siewert (1993a), who changed the space variable in Eq. (11) to an optical variable measured in units of the largest of the mean free paths $\{1/\sigma_i\}$. In this paper, to facilitate the coupling between the scalar and vector P_N methods, we prefer to work directly with Eq. (11). Associated with Eq. (11), we consider the boundary conditions, for $\mu \in (0, 1]$,

$$\mathbf{\Psi}(z_L,\mu) = \mathbf{L}(\mu) \tag{15a}$$

and

$$\mathbf{\Psi}(z_R,-\mu) = \mathbf{R}(\mu), \tag{15b}$$

where the known vectors of incident distributions are defined as

$$\mathbf{L}(\mu) = \begin{pmatrix} L_{G_d+1}(\mu) \\ L_{G_d+2}(\mu) \\ \vdots \\ L_G(\mu) \end{pmatrix} \tag{16a}$$

and

$$\mathbf{R}(\mu) = \begin{pmatrix} R_{G_d+1}(\mu) \\ R_{G_d+2}(\mu) \\ \vdots \\ R_G(\mu) \end{pmatrix}. \tag{16b}$$

Proceeding with our presentation, we follow Siewert (1993a) and write our P_N solution to Eq. (11) as

$$\mathbf{\Psi}(z,\mu) = \mathbf{\Psi}^h(z,\mu) + \mathbf{\Psi}^p(z,\mu), \tag{17}$$

where $\mathbf{\Psi}^h(z,\mu)$ denotes the P_N solution to the homogeneous version of Eq. (11) and $\mathbf{\Psi}^p(z,\mu)$ denotes a particular P_N solution to Eq. (11). The homogenous solution satisfies the first $N+1$ angular moments of Eq. (11) with $\mathbf{Q}(z,\mu) = \mathbf{0}$ and is given by

$$\mathbf{\Psi}^h(z,\mu) = \frac{1}{2}\sum_{n=0}^{N}(2n+1)\mathbf{\Phi}_n^h(z)P_n(\mu), \tag{18}$$

where

$$\mathbf{\Phi}_n^h(z) = \sum_{j=1}^{J}\left[A_j \mathrm{e}^{-(z-z_L)/\xi_j} + (-1)^n B_j \mathrm{e}^{-(z_R-z)/\xi_j}\right]\mathbf{T}_n(\xi_j), \tag{19}$$

with $J = G_u \times (N+1)/2$. Here, the polynomial vectors $\{\mathbf{T}_n(\xi)\}$ obey the recurrence formula

$$\xi \mathbf{h}_n \mathbf{T}_n(\xi) = (n+1)\mathbf{T}_{n+1}(\xi) + n\mathbf{T}_{n-1}(\xi), \tag{20}$$

where

$$\mathbf{h}_n = \begin{cases} (2n+1)\mathbf{\Sigma} - \mathbf{C}_n, & n \le \mathcal{L}, \\ (2n+1)\mathbf{\Sigma}, & n > \mathcal{L}, \end{cases} \tag{21}$$

and the P_N eigenvalues $\{\pm\xi_j\}$ are the J $\pm$ pairs of the parameter ξ that satisfy the truncation condition $\mathbf{T}_{N+1}(\xi) = \mathbf{0}$.

It can be shown that the determination of the required P_N eigenvalues and associated $\mathbf{T}$-vectors can be reduced to the problem of solving the eigensystem (Siewert and Thomas, 1987; Siewert, 1993a)

$$\mathbf{A}\mathbf{T}_e(\xi) = \xi^2 \mathbf{T}_e(\xi), \tag{22}$$

where the $J \times J$ matrix $\mathbf{A}$ has the structure

$$\mathbf{A} = \begin{pmatrix} \mathbf{Y}_0 & \mathbf{Z}_0 & \mathbf{0} & \dots & \mathbf{0} & \mathbf{0} & \mathbf{0} \\ \mathbf{X}_2 & \mathbf{Y}_2 & \mathbf{Z}_2 & \dots & \mathbf{0} & \mathbf{0} & \mathbf{0} \\ \mathbf{0} & \mathbf{X}_4 & \mathbf{Y}_4 & \dots & \mathbf{0} & \mathbf{0} & \mathbf{0} \\ \vdots & \vdots & \vdots & \ddots & \vdots & \vdots & \vdots \\ \mathbf{0} & \mathbf{0} & \mathbf{0} & \dots & \mathbf{Y}_{N-5} & \mathbf{Z}_{N-5} & \mathbf{0} \\ \mathbf{0} & \mathbf{0} & \mathbf{0} & \dots & \mathbf{X}_{N-3} & \mathbf{Y}_{N-3} & \mathbf{Z}_{N-3} \\ \mathbf{0} & \mathbf{0} & \mathbf{0} & \dots & \mathbf{0} & \mathbf{X}_{N-1} & \mathbf{Y}_{N-1} \end{pmatrix}, \tag{23}$$

with

$$\mathbf{X}_n = n(n-1)\mathbf{h}_n^{-1}\mathbf{h}_{n-1}^{-1}, \tag{24a}$$

$$\mathbf{Y}_n = n^2\mathbf{h}_n^{-1}\mathbf{h}_{n-1}^{-1} + (n+1)^2\mathbf{h}_n^{-1}\mathbf{h}_{n+1}^{-1} \tag{24b}$$

and

$$\mathbf{Z}_n = (n+1)(n+2)\mathbf{h}_n^{-1}\mathbf{h}_{n+1}^{-1}, \tag{24c}$$

and the vector $\mathbf{T}_e(\xi)$ of dimension J has the even $\mathbf{T}$-vectors as subvector components, i.e.

$$\mathbf{T}_e(\xi) = \begin{pmatrix} \mathbf{T}_0(\xi) \\ \mathbf{T}_2(\xi) \\ \vdots \\ \mathbf{T}_{N-1}(\xi) \end{pmatrix}. \tag{25}$$

Once the eigensystem expressed by Eq. (22) is solved, the required $\{\xi_j\}$ can be found as the *positive* square roots of the eigenvalues and $\mathbf{T}_n(\xi_j)$, $n = 0, 2, \ldots, N-1$, as the subvector components of the associated eigenvectors, according to Eq. (25). Of course, once the even $\mathbf{T}$-vectors are established, the odd ones can be computed by using Eq. (20) with $n = 1, 3, \ldots, N$ and the truncation condition $\mathbf{T}_{N+1}(\xi_j) = \mathbf{0}$.

We note that the problem of computing the P_N eigenvalues and eigenvectors can also be formulated in terms of the odd $\mathbf{T}$-vectors. In this alternative formulation, we have to solve (Siewert, 1993a)

$$\mathbf{B}\mathbf{T}_o(\xi) = \xi^2\mathbf{T}_o(\xi), \tag{26}$$

where the $J \times J$ matrix $\mathbf{B}$ has the structure

$$\mathbf{B} = \begin{pmatrix} \mathbf{Y}_1 & \mathbf{Z}_1 & \mathbf{0} & \ldots & \mathbf{0} & \mathbf{0} & \mathbf{0} \\ \mathbf{X}_3 & \mathbf{Y}_3 & \mathbf{Z}_3 & \ldots & \mathbf{0} & \mathbf{0} & \mathbf{0} \\ \mathbf{0} & \mathbf{X}_5 & \mathbf{Y}_5 & \ldots & \mathbf{0} & \mathbf{0} & \mathbf{0} \\ \vdots & \vdots & \vdots & \ddots & \vdots & \vdots & \vdots \\ \mathbf{0} & \mathbf{0} & \mathbf{0} & \ldots & \mathbf{Y}_{N-4} & \mathbf{Z}_{N-4} & \mathbf{0} \\ \mathbf{0} & \mathbf{0} & \mathbf{0} & \ldots & \mathbf{X}_{N-2} & \mathbf{Y}_{N-2} & \mathbf{Z}_{N-2} \\ \mathbf{0} & \mathbf{0} & \mathbf{0} & \ldots & \mathbf{0} & \mathbf{X}_N & \mathbf{Y}'_N \end{pmatrix}, \tag{27}$$

with

$$\mathbf{Y}'_N = N^2\mathbf{h}_N^{-1}\mathbf{h}_{N-1}^{-1}, \tag{28}$$

and the vector $\mathbf{T}_o(\xi)$ of dimension J has the odd $\mathbf{T}$-vectors as subvector components, i.e.

$$\mathbf{T}_o(\xi) = \begin{pmatrix} \mathbf{T}_1(\xi) \\ \mathbf{T}_3(\xi) \\ \vdots \\ \mathbf{T}_N(\xi) \end{pmatrix}. \tag{29}$$

Again, once the eigensystem defined by Eq. (26) is solved, the required $\{\xi_j\}$ can be found as the positive square roots of the eigenvalues, the required odd $\mathbf{T}$-vectors can be found as the subvector components of the associated eigenvectors, according to Eq. (29), and the required even $\mathbf{T}$-vectors can be computed from Eq. (20) with $n = 0, 2, \ldots, N-1$.

To complete our P_N solution defined by Eq. (17), we now make use of a particular P_N solution developed by Siewert (1993a). We note that his solution satisfies the first $N+1$ angular moments of Eq. (11) and can be written as

$$\mathbf{\Psi}^p(z,\mu) = \frac{1}{2}\sum_{n=0}^{N}(2n+1)\mathbf{\Phi}_n^p(z)P_n(\mu), \tag{30}$$

where

$$\mathbf{\Phi}_n^p(z) = \sum_{j=1}^{J}\frac{C_j}{\xi_j}[U_j(z) + (-1)^n V_j(z)]\mathbf{T}_n(\xi_j). \tag{31}$$

Here

$$C_j = \left(\sum_{k=1}^{K} \tilde{\mathbf{T}}^{\dagger}_{2k-2}(\xi_j) \mathbf{h}_{2k-2} \mathbf{T}_{2k-2}(\xi_j) \right)^{-1}, \tag{32}$$

where the tilde denotes the transpose operation and the $\{\mathbf{T}^{\dagger}_n(\xi_j)\}$ satisfy the recurrence formula

$$\xi \tilde{\mathbf{h}}_n \mathbf{T}^{\dagger}_n(\xi) = (n+1)\mathbf{T}^{\dagger}_{n+1}(\xi) + n\mathbf{T}^{\dagger}_{n-1}(\xi) \tag{33}$$

for $n = 0, 1, \ldots, N$ and the truncation condition $\mathbf{T}^{\dagger}_{N+1}(\xi_j) = \mathbf{0}$ for $j = 1, 2, \ldots, J$, and are related (Siewert, 1993a) to the left eigenvectors of the matrices $\mathbf{A}$ and $\mathbf{B}$ defined respectively by Eqs. (23) and (27). Moreover,

$$U_j(z) = \int_{z_L}^{z} u_j(z') \mathrm{e}^{-(z-z')/\xi_j} \mathrm{d}z' \tag{34a}$$

and

$$V_j(z) = \int_{z}^{z_R} v_j(z') \mathrm{e}^{-(z'-z)/\xi_j} \mathrm{d}z', \tag{34b}$$

with

$$u_j(z) = \sum_{n=0}^{N} \tilde{\mathbf{T}}^{\dagger}_n(\xi_j) \mathbf{Q}_n(z) \tag{35a}$$

and

$$v_j(z) = \sum_{n=0}^{N} (-1)^n \tilde{\mathbf{T}}^{\dagger}_n(\xi_j) \mathbf{Q}_n(z), \tag{35b}$$

where

$$\mathbf{Q}_n(z) = \frac{1}{2}(2n+1) \int_{-1}^{1} \mathbf{Q}(z, \mu) P_n(\mu) \mathrm{d}\mu. \tag{36}$$

Finally, as for the scalar problems, the coefficients $\{A_j\}$ and $\{B_j\}$ in Eq. (19) are to be determined from the boundary conditions. Using the Mark version of the boundary conditions expressed by Eq. (15a) and (15b) and introducing the vectors

$$\mathbf{X}(\xi, \mu) = \frac{1}{2} \sum_{n=0}^{N} (2n+1) \mathbf{T}_n(\xi) P_n(\mu) \tag{37a}$$

and

$$\mathbf{Y}(\xi, \mu) = \frac{1}{2} \sum_{n=0}^{N} (-1)^n (2n+1) \mathbf{T}_n(\xi) P_n(\mu), \tag{37b}$$

we find the linear system of equations

$$\sum_{j=1}^{J} \left[A_j \mathbf{X}(\xi_j, \mu_m) + B_j \mathbf{Y}(\xi_j, \mu_m) \mathrm{e}^{-\Delta/\xi_j} \right] = \mathbf{L}(\mu_m) - \boldsymbol{\Psi}^p(z_L, \mu_m) \tag{38a}$$

and

$$\sum_{j=1}^{J} \left[B_j \mathbf{X}(\xi_j, \mu_m) + A_j \mathbf{Y}(\xi_j, \mu_m) \mathrm{e}^{-\Delta/\xi_j} \right] = \mathbf{R}(\mu_m) - \boldsymbol{\Psi}^p(z_R, -\mu), \tag{38b}$$

for $m = 1, 2, \ldots, K$, that is to be solved for $\{A_j\}$ and $\{B_j\}$. Once these coefficients become available, we can compute P_N approximations to some quantities of physical interest. We begin with the vector of thermal scalar fluxes $\boldsymbol{\phi}(z)$ which is given by the sum of Eqs. (19) and (31) for $n = 0$. We obtain

$$\boldsymbol{\phi}(z) = \sum_{j=1}^{J} \left[A_j \mathrm{e}^{-(z-z_L)/\xi_j} + B_j \mathrm{e}^{-(z_R-z)/\xi_j} + \frac{C_j}{\xi_j} [U_j(z) + V_j(z)] \right] \mathbf{T}_0(\xi_j). \tag{39}$$

Similarly, adding Eqs. (19) and (31) for $n = 1$, we find that the vector of thermal currents $\mathbf{J}(z)$ is given by

$$\mathbf{J}(z) = \sum_{j=1}^{J} \left[A_j \mathrm{e}^{-(z-z_L)/\xi_j} - B_j \mathrm{e}^{-(z_R-z)/\xi_j} + \frac{C_j}{\xi_j}[U_j(z) - V_j(z)] \right] \mathbf{T}_1(\xi_j). \tag{40}$$

We can also generalize the one-group result of Garcia and Siewert (1996) to find that the vectors of partial currents $\mathbf{J}^+(z)$ and $\mathbf{J}^-(z)$ can be expressed as

$$\mathbf{J}^{\pm}(z) = \frac{1}{4}\boldsymbol{\phi}(z) \pm \frac{1}{2}\mathbf{J}(z) - \frac{1}{2}\sum_{k=1}^{K-1}(-1)^k(4k+1)\frac{(2k-3)!!}{(2k+2)!!}\boldsymbol{\Phi}_{2k}(z), \tag{41}$$

where the definition $(-1)!! = 1$ is to be used and

$$\boldsymbol{\Phi}_{2k}(z) = \boldsymbol{\Phi}^h_{2k}(z) + \boldsymbol{\Phi}^p_{2k}(z). \tag{42}$$

Finally, in regard to the vector of thermal angular fluxes, we can use the source-function integration technique in the manner of Siewert (1993a) to find the postprocessed results, for $\mu \in [0, 1]$,

$$\begin{aligned}\boldsymbol{\Psi}(z,\mu) &= \mathrm{e}^{-\boldsymbol{\Sigma}(z-z_L)/\mu}\,\mathbf{L}(\mu) + \frac{1}{\mu}\int_{z_L}^{z} \mathrm{e}^{-\boldsymbol{\Sigma}(z-z')/\mu}\mathbf{Q}(z',\mu)\mathrm{d}z' + \boldsymbol{\Xi}(z,\mu) \\ &\quad + \sum_{j=1}^{J} \xi_j \left[A_j \mathbf{C}(z - z_L : \mu\boldsymbol{\Sigma}^{-1}, \xi_j)\mathbf{M}(\xi_j,\mu) + B_j \mathrm{e}^{-(z_R-z)/\xi_j}\mathbf{S}(z - z_L : \mu\boldsymbol{\Sigma}^{-1}, \xi_j)\mathbf{N}(\xi_j,\mu) \right] \end{aligned} \tag{43a}$$

and

$$\begin{aligned}\boldsymbol{\Psi}(z,-\mu) &= \mathrm{e}^{-\boldsymbol{\Sigma}(z_R-z)/\mu}\,\mathbf{R}(\mu) + \frac{1}{\mu}\int_{z}^{z_R} \mathrm{e}^{-\boldsymbol{\Sigma}(z'-z)/\mu}\mathbf{Q}(z',-\mu)\mathrm{d}z' + \boldsymbol{\Xi}(z,-\mu) \\ &\quad + \sum_{j=1}^{J} \xi_j \left[A_j \mathrm{e}^{-(z-z_L)/\xi_j}\mathbf{S}(z_R - z : \mu\boldsymbol{\Sigma}^{-1}, \xi_j)\mathbf{N}(\xi_j,\mu) + B_j \mathbf{C}(z_R - z : \mu\boldsymbol{\Sigma}^{-1}, \xi_j)\mathbf{M}(\xi_j,\mu) \right], \end{aligned} \tag{43b}$$

where

$$\mathbf{M}(\xi,\mu) = \frac{1}{2}\boldsymbol{\Sigma}^{-1}\sum_{\ell=0}^{\mathcal{L}} \mathbf{C}_\ell \mathbf{T}_\ell(\xi) P_\ell(\mu) \tag{44a}$$

and

$$\mathbf{N}(\xi,\mu) = \frac{1}{2}\boldsymbol{\Sigma}^{-1}\sum_{\ell=0}^{\mathcal{L}} (-1)^\ell \mathbf{C}_\ell \mathbf{T}_\ell(\xi) P_\ell(\mu), \tag{44b}$$

and where

$$\mathbf{C}(z : \mu\boldsymbol{\Sigma}^{-1}, \xi) = \mathrm{diag}\{C(z : \mu/\sigma_{G_d+1}, \xi), C(z : \mu/\sigma_{G_d+2}, \xi), \ldots, C(z : \mu/\sigma_G, \xi)\} \tag{45a}$$

and

$$\mathbf{S}(z : \mu\boldsymbol{\Sigma}^{-1}, \xi) = \mathrm{diag}\{S(z : \mu/\sigma_{G_d+1}, \xi), S(z : \mu/\sigma_{G_d+2}, \xi), \ldots, S(z : \mu/\sigma_G, \xi)\}, \tag{45b}$$

with

$$C(z : \mu, \xi) = \frac{\mathrm{e}^{-z/\mu} - \mathrm{e}^{-z/\xi}}{\mu - \xi} \tag{46a}$$

and

$$S(z : \mu, \xi) = \frac{1 - \mathrm{e}^{-z/\mu}\,\mathrm{e}^{-z/\xi}}{\mu + \xi}. \tag{46b}$$

In addition, the vectors $\boldsymbol{\Xi}(z, \pm\mu)$ required in Eqs. (43a) and (43b) are given by

$$\begin{aligned}\boldsymbol{\Xi}(z,\mu) &= \sum_{j=1}^{J} C_j \left\{ \left[\int_{z_L}^{z} u_j(z')\mathbf{C}(z - z' : \mu\boldsymbol{\Sigma}^{-1}, \xi_j)\mathrm{d}z' \right] \mathbf{M}(\xi_j,\mu) \right. \\ &\quad \left. + \left[V_j(z)\mathbf{S}(z - z_L : \mu\boldsymbol{\Sigma}^{-1}, \xi_j) + \int_{z_L}^{z} v_j(z')\mathrm{e}^{-\boldsymbol{\Sigma}(z-z')/\mu}\mathbf{S}(z' - z_L : \mu\boldsymbol{\Sigma}^{-1}, \xi_j)\mathrm{d}z' \right] \mathbf{N}(\xi_j,\mu) \right\} \end{aligned} \tag{47a}$$

and

$$\begin{aligned}\boldsymbol{\Xi}(z,-\mu) &= \sum_{j=1}^{J} C_j \left\{ \left[\int_{z}^{z_R} v_j(z')\mathbf{C}(z' - z : \mu\boldsymbol{\Sigma}^{-1}, \xi_j)\mathrm{d}z' \right] \mathbf{M}(\xi_j,\mu) \right. \\ &\quad \left. + \left[U_j(z)\mathbf{S}(z_R - z : \mu\boldsymbol{\Sigma}^{-1}, \xi_j) + \int_{z}^{z_R} u_j(z')\mathrm{e}^{-\boldsymbol{\Sigma}(z'-z)/\mu}\mathbf{S}(z_R - z' : \mu\boldsymbol{\Sigma}^{-1}, \xi_j)\mathrm{d}z' \right] \mathbf{N}(\xi_j,\mu) \right\}. \end{aligned} \tag{47b}$$

4. Coupling the scalar and vector P_N methods

In this section, we work out the details of our way of coupling the scalar and vector P_N methods summarized in Sections 2 and 3. As already mentioned in the Introduction, the link of coupling between these methods consists of the downscatter sources from the fast and epithermal groups $\alpha = 1, 2, \ldots, G_d$ to the thermal groups $i = G_d + 1, G_d + 2, \ldots, G$. Considering $N \geq \mathcal{L}$, we find that the source vector $\mathbf{Q}(z, \mu)$ in Eq. (11) has the components

$$Q_i(z, \mu) = \frac{1}{2} \sum_{\ell=0}^{\mathcal{L}} P_\ell(\mu) \sum_{\alpha=1}^{G_d} \sigma_{i\alpha}(\ell) \phi_{\alpha,\ell}(z), \tag{48}$$

which, in view of Eq. (5), can be written in a more explicit form as

$$Q_i(z, \mu) = \frac{1}{2} \sum_{\ell=0}^{\mathcal{L}} P_\ell(\mu) \sum_{\alpha=1}^{G_d} \sigma_{i\alpha}(\ell) \sum_{\beta=1}^{\alpha} \sum_{k=1}^{K} \left[A_{\beta,k} \mathrm{e}^{-\sigma_\beta (z - z_L)/\xi_{\beta,k}} + (-1)^\ell B_{\beta,k} \mathrm{e}^{-\sigma_\beta (z_R - z)/\xi_{\beta,k}} \right] g_\ell^{\alpha\beta}(\xi_{\beta,k}), \tag{49}$$

for $i = G_d + 1, G_d + 2, \ldots, G$. Clearly, since the source vector $\mathbf{Q}(z, \mu)$ is explicitly known so are the moments $\{\mathbf{Q}_n(z)\}$ defined by Eq. (36). Thus, we can use these moments in Eqs. (35a) and (35b) to find explicit expressions for the quantities $\{U_j(z)\}$ and $\{V_j(z)\}$ defined respectively by Eqs. (34a) and (34b) and required to establish our particular P_N solution to Eq. (11). After inverting the order of the summations in α and β in the resulting expressions, we find, for $j = 1, 2, \ldots, J$,

$$U_j(z) = \sum_{m=G_d+1}^{G} \sum_{\ell=0}^{\mathcal{L}} T_{\ell,m}^\dagger(\xi_j) \sum_{\beta=1}^{G_d} \sum_{\alpha=\beta}^{G_d} \sigma_{m\alpha}(\ell) \epsilon_\ell^{\alpha\beta}(z - z_L, \xi_j) \tag{50a}$$

and

$$V_j(z) = \sum_{m=G_d+1}^{G} \sum_{\ell=0}^{\mathcal{L}} (-1)^\ell T_{\ell,m}^\dagger(\xi_j) \sum_{\beta=1}^{G_d} \sum_{\alpha=\beta}^{G_d} \sigma_{m\alpha}(\ell) \lambda_\ell^{\alpha\beta}(z_R - z, \xi_j), \tag{50b}$$

where $T_{\ell,m}^\dagger(\xi)$ denotes the $(m - G_d)$'th component of the vector $\mathbf{T}_\ell^\dagger(\xi)$, and we have used the definitions

$$\epsilon_\ell^{\alpha\beta}(z, \zeta) = \frac{\zeta}{2} \sum_{k=1}^{K} (\xi_{\beta,k}/\sigma_\beta) \left[A_{\beta,k} C(z : \xi_{\beta,k}/\sigma_\beta, \zeta) + (-1)^\ell B_{\beta,k} \mathrm{e}^{-\sigma_\beta(\Delta - z)/\xi_{\beta,k}} S(z : \xi_{\beta,k}/\sigma_\beta, \zeta) \right] g_\ell^{\alpha\beta}(\xi_{\beta,k}) \tag{51a}$$

and

$$\lambda_\ell^{\alpha\beta}(z, \zeta) = \frac{\zeta}{2} \sum_{k=1}^{K} (\xi_{\beta,k}/\sigma_\beta) \left[A_{\beta,k} \mathrm{e}^{-\sigma_\beta(\Delta - z)/\xi_{\beta,k}} S(z : \xi_{\beta,k}/\sigma_\beta, \zeta) + (-1)^\ell B_{\beta,k} C(z : \xi_{\beta,k}/\sigma_\beta, \zeta) \right] g_\ell^{\alpha\beta}(\xi_{\beta,k}). \tag{51b}$$

Now that the quantities $\{U_j(z)\}$ and $\{V_j(z)\}$ are available, we can write our postprocessed results for the thermal angular fluxes expressed by Eqs. (43a) and (43b) in more detail. Indeed, after some algebra, we can show that the vector quantities $\Xi(z, \pm\mu)$, $\mu \in [0, 1]$, that appear in these equations have the components, for $i = G_d + 1, G_d + 2, \ldots, G$,

$$\begin{aligned} \Xi_i(z, \mu) = \sum_{m=G_d+1}^{G} \sum_{j=1}^{J} C_j \sum_{\ell=0}^{\mathcal{L}} T_{\ell,m}^\dagger(\xi_j) \sum_{\beta=1}^{G_d} \sum_{\alpha=\beta}^{G_d} \sigma_{m\alpha}(\ell) \Bigg\{ & \left[\frac{\epsilon_\ell^{\alpha\beta}(z - z_L, \mu/\sigma_i) - \epsilon_\ell^{\alpha\beta}(z - z_L, \xi_j)}{(\mu/\sigma_i) - \xi_j} \right] M_i(\xi_j, \mu) \\ & + (-1)^\ell \Bigg\{ \lambda_\ell^{\alpha\beta}(z_R - z, \xi_j) S(z - z_L : \mu/\sigma_i, \xi_j) \\ & + \left[\frac{\epsilon_\ell^{\alpha\beta}(z - z_L, \mu/\sigma_i) - \mathrm{e}^{-\sigma_i (z - z_L)/\mu} \varphi_\ell^{\alpha\beta}(z - z_L, \xi_j)}{(\mu/\sigma_i) + \xi_j} \right] \Bigg\} N_i(\xi_j, \mu) \Bigg\} \end{aligned} \tag{52a}$$

and

$$\Xi_i(z,-\mu) = \sum_{m=G_d+1}^{G}\sum_{j=1}^{J} C_j \sum_{\ell=0}^{\mathcal{L}} T^{\dagger}_{\ell,m}(\xi_j) \sum_{\beta=1}^{G_d}\sum_{\alpha=\beta}^{G_d} \sigma_{m\alpha}(\ell)\Bigg\{(-1)^{\ell}\left[\frac{\lambda_{\ell}^{\alpha\beta}(z_R-z,\mu/\sigma_i)-\lambda_{\ell}^{\alpha\beta}(z_R-z,\xi_j)}{(\mu/\sigma_i)-\xi_j}\right] \times M_i(\xi_j,\mu) + \Bigg\{\epsilon_{\ell}^{\alpha\beta}(z-z_L,\xi_j)S(z_R-z:\mu/\sigma_i,\xi_j) + \left[\frac{\lambda_{\ell}^{\alpha\beta}(z_R-z,\mu/\sigma_i)-\mathrm{e}^{-\sigma_i(z_R-z)/\mu}\chi_{\ell}^{\alpha\beta}(z_R-z,\xi_j)}{(\mu/\sigma_i)+\xi_j}\right]\Bigg\} N_i(\xi_j,\mu)\Bigg\}, \quad (52b)$$

where

$$M_i(\xi,\mu) = \left(\frac{1}{2\sigma_i}\right)\sum_{\ell=0}^{\mathcal{L}} P_{\ell}(\mu) \sum_{m=G_d+1}^{G} \sigma_{im}(\ell) T_{\ell,m}(\xi) \quad (53a)$$

and

$$N_i(\xi,\mu) = \left(\frac{1}{2\sigma_i}\right)\sum_{\ell=0}^{\mathcal{L}} (-1)^{\ell} P_{\ell}(\mu) \sum_{m=G_d+1}^{G} \sigma_{im}(\ell) T_{\ell,m}(\xi) \quad (53b)$$

are the $(i-G_d)$'th components of the vectors $\mathbf{M}(\xi,\mu)$ and $\mathbf{N}(\xi_j,\mu)$, respectively, and we have used the additional definitions

$$\varphi_{\ell}^{\alpha\beta}(z,\zeta) = \frac{\zeta}{2}\sum_{k=1}^{K}(\xi_{\beta,k}/\sigma_{\beta})\left[A_{\beta,k}S(z:\xi_{\beta,k}/\sigma_{\beta},\zeta) + (-1)^{\ell}B_{\beta,k}\mathrm{e}^{-\sigma_{\beta}(\Delta-z)/\xi_{\beta,k}}C(z:\xi_{\beta,k}/\sigma_{\beta},\zeta)\right] g_{\ell}^{\alpha\beta}(\xi_{\beta,k}) \quad (54a)$$

and

$$\chi_{\ell}^{\alpha\beta}(z,\zeta) = \frac{\zeta}{2}\sum_{k=1}^{K}(\xi_{\beta,k}/\sigma_{\beta})\left[A_{\beta,k}\mathrm{e}^{-\sigma_{\beta}(\Delta-z)/\xi_{\beta,k}}C(z:\xi_{\beta,k}/\sigma_{\beta},\zeta) + (-1)^{\ell}B_{\beta,k}S(z:\xi_{\beta,k}/\sigma_{\beta},\zeta)\right] g_{\ell}^{\alpha\beta}(\xi_{\beta,k}). \quad (54b)$$

In addition, we can readily show that the source integral vectors in Eqs. (43a) and (43b) have, respectively, the components, for $i = G_d+1, G_d+2, \ldots, G$,

$$\int_{z_L}^{z} \mathrm{e}^{-\sigma_i(z-z')/\mu} Q_i(z',\mu)\mathrm{d}z' = \sum_{\ell=0}^{\mathcal{L}} P_{\ell}(\mu) \sum_{\beta=1}^{G_d}\sum_{\alpha=\beta}^{G_d} \sigma_{i\alpha}(\ell)\epsilon_{\ell}^{\alpha\beta}(z-z_L,\mu/\sigma_i) \quad (55a)$$

and

$$\int_{z}^{z_R} \mathrm{e}^{-\sigma_i(z'-z)/\mu} Q_i(z',-\mu)\mathrm{d}z' = \sum_{\ell=0}^{\mathcal{L}} (-1)^{\ell} P_{\ell}(\mu) \sum_{\beta=1}^{G_d}\sum_{\alpha=\beta}^{G_d} \sigma_{i\alpha}(\ell)\lambda_{\ell}^{\alpha\beta}(z_R-z,\mu/\sigma_i), \quad (55b)$$

for $\mu \in [0,1]$. With the formulas reported in this section, we consider that our coupled P_N solution is now completely defined.

5. Extension to multislab geometry

So far in this paper we have treated only multigroup problems formulated as a single slab. Our extension of the method to multislab geometry that is described in this section relies on an iterative approach which is based on solving the problem one slab at a time and using spatial sweeps to connect these solutions and guide them to convergence. Although the P_N method can be formulated in a way that permits solution of multislab problems without iteration, we believe that the iterative approach adopted here has the merit of being less limited by computational resources.

To explain our way of solving multigroup transport problems in multislab geometry, we consider a system of R slabs, as shown in Fig. 1. We assume, as before, that the group structure has a total of $G = G_d + G_u$ energy groups, with G_d denoting the number of fast and epithermal groups and G_u the number of thermal groups. On the left and right boundaries of the system, the incident distributions of radiation are specified, respectively, by the vectors $\mathbf{L}(\mu)$ and $\mathbf{R}(\mu)$ of G components. The problem here is to find P_N approximations

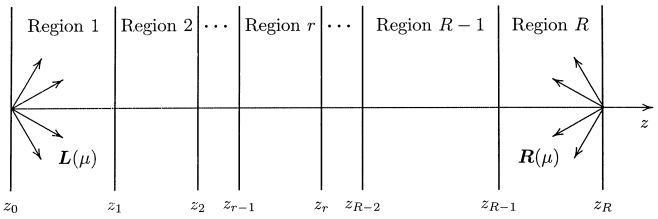

Fig. 1. A system of R slabs in multislab geometry

to the vector of angular fluxes $\mathbf{\Psi}_r(z,\mu)$, $z \in (z_{r-1}, z_r)$ and $\mu \in [-1,1]$, and related integral quantities, for the regions $r = 1, 2, \ldots, R$, given the boundary and interface conditions, for $\mu \in (0,1]$,

$$\mathbf{\Psi}_1(z_0,\mu) = \mathbf{L}(\mu), \tag{56a}$$

$$\mathbf{\Psi}_r(z_r,\pm\mu) = \mathbf{\Psi}_{r+1}(z_r,\pm\mu), \quad r = 1,2,\ldots,R-1, \tag{56b}$$

and

$$\mathbf{\Psi}_R(z_R,-\mu) = \mathbf{R}(\mu). \tag{56c}$$

We now describe our sweep procedure. First of all, we note that, for any region r, the first G_d components of the angular-flux vector, $\Psi_{r,1}(z,\mu), \Psi_{r,2}(z,\mu), \ldots, \Psi_{r,G_d}(z,\mu)$, are solved using the scalar P_N method summarized in Section 2, while the remaining G_u components $\Psi_{r,G_d+1}(z,\mu), \Psi_{r,G_d+2}(z,\mu), \ldots, \Psi_{r,G}(z,\mu)$ are solved using the vector P_N method coupled to the scalar method as discussed in Section 4. The first sweep is initiated at the leftmost slab ($r = 1$) and proceeds by solving the problem for all subsequent slabs $r = 2, 3, \ldots, R$. After the problem for the rightmost slab ($r = R$) has been solved, the sweep direction is reversed and the problems for slabs $r = R-1, R-2, \ldots, 1$ are solved again with updated boundary conditions, as explained next. This sequence of right/left sweeps is repeated as many times as necessary for convergence in the solution. In any of these sweeps, the problem for slab r is formulated as being subject to the boundary conditions, for $\mu \in (0,1]$,

$$\mathbf{\Psi}_r(z_{r-1},\mu) = \mathbf{L}_r(\mu) \tag{57a}$$

and

$$\mathbf{\Psi}_r(z_r,-\mu) = \mathbf{R}_r(\mu), \tag{57b}$$

where the vectors $\mathbf{L}_r(\mu)$ and $\mathbf{R}_r(\mu)$ are either known, initialized in an arbitrary way or approximated by the result of the previous sweep. Clearly, $\mathbf{L}_1(\mu)$ and $\mathbf{R}_R(\mu)$ are known for all sweeps and are given by the incident distributions of radiation, i.e.

$$\mathbf{L}_1(\mu) = \mathbf{L}(\mu) \tag{58a}$$

and

$$\mathbf{R}_R(\mu) = \mathbf{R}(\mu). \tag{58b}$$

In addition, when the sweep is to the left we use, for $\mu \in (0,1]$,

$$\mathbf{L}_r(\mu) = \mathbf{\Psi}^p_{r-1}(z_{r-1},\mu), \quad r = 2,3,\ldots,R, \tag{59a}$$

and

$$\mathbf{R}_r(\mu) = \mathbf{\Psi}^c_{r+1}(z_r,-\mu), \quad r = 1,2,\ldots,R-1, \tag{59b}$$

where the superscripts c and p indicate angular-flux vectors computed in the *current* and the *previous* sweep, respectively. Similarly, when the sweep is to the right, we use, for $\mu \in (0, 1]$,

$$\mathbf{L}_r(\mu) = \mathbf{\Psi}^c_{r-1}(z_{r-1}, \mu), \quad r = 2, 3, \ldots, R, \tag{60a}$$

and

$$\mathbf{R}_r(\mu) = \mathbf{\Psi}^p_{r+1}(z_r, -\mu), \quad r = 1, 2, \ldots, R-1, \tag{60b}$$

except when the sweep is the first, in which case we make use of the arbitrary initialization $\mathbf{R}_r(\mu) = \mathbf{0}$, $r = 1, 2, \ldots, R-1$, in place of Eq. (60b).

Finally, to stop the sweep process, we have adopted the criterion that the maximum relative deviation displayed in two consecutive sweeps by the exit fluxes $\mathbf{\Psi}_1(z_0, -\mu_m)$ and $\mathbf{\Psi}_R(z_R, \mu_m)$ and the interface fluxes $\mathbf{\Psi}_r(z_r, \pm\mu_m)$, $r = 1, 2, \ldots, R-1$, where $\{\mu_m\}$ are the Mark points defined in Section 2, should not exceed a prescribed amount (10^{-6} was our choice for the first and third problems discussed in the forthcoming section).

6. Test problems

To evaluate and compare the performance of the scalar, vector and coupled P_N methods, several test problems (Dias, 1999) were solved in the course of this study. Here, we report numerical results for three such problems. The first is a five-region, 20-group, downscatter-only problem with synthetic cross sections and scattering anisotropy of 10th order that was introduced some years ago (Garcia and Siewert, 1983) to test the F_N method for solving multigroup slowing-down problems in multislab geometry. The second (Garcia and Siewert, 1998) consists of a concrete slab with linearly anisotropic scattering and group constants defined in the WIMS 42-group thermal structure, and the third is a one-dimensional model of a fast-reactor shield (Dias and Ono, 1995) that comprises seven regions, scattering anisotropy of 7th order and a 25-group structure (21 groups for neutrons and 4 for gammas).

6.1 Five-region, 20-group, downscatter-only problem

Following Garcia and Siewert (1983) and referring to Fig. 1 with $R = 5$, we can specify this problem by taking $\Delta_r = z_r - z_{r-1} = (r + 1)$ cm, for $r = 1, 2, \ldots, 5$, and using the synthetic cross-section set (in units of cm^{-1}), for $r = 1, 2, \ldots, 5$ and $i = 1, 2, \ldots, 20$,

$$\sigma^r_i = \left(\frac{r + 20}{21}\right)^5 [0.1 \times i - 0.15(\delta_{i,5} + \delta_{i,10})] \tag{61a}$$

and

$$\sigma^r_{ij}(\ell) = (2\ell + 1)\left(\frac{r + 20}{21}\right)\left[\frac{j}{100(i - j + 1)}\right](g_{ij})^\ell, \quad j = 1, 2, \ldots, i \text{ and } \ell = 0, 1, \ldots, 10, \tag{61b}$$

with $g_{ij} = 0.7 - (i + j)/200$. In addition, the boundary conditions for this problem are such that we have an isotropic distribution of radiation impinging uniformly on the left boundary z_0 only in the highest (first) energy group, i.e.

$$\mathbf{L}(\mu) = \begin{pmatrix} 1 & 0 & \ldots & 0 \end{pmatrix}^T, \tag{62a}$$

and a vacuum boundary at z_5, i.e.

$$\mathbf{R}(\mu) = \mathbf{0}. \tag{62b}$$

This problem was solved using the purely scalar and vector methods, as well as the coupled method with $G_d = 10$ and $G_u = 10$, for the purpose of comparing the computational efficiency of these three methods. In Tables 1 and 2, we list the group albedos $A^*_i = J^-_i(z_0)/J^+_1(z_0)$ and transmission factors $B^*_i = J^+_i(z_5)/J^+_1(z_0)$ for $i = 1, 2, \ldots, 20$ and several orders of the P_N approximation, along with the reference F_N results of Garcia and Siewert (1983).

Table 1
The group albedos A_i^* for the five-region, 20-group, downscatter-only problem

i	$N = 19$	$N = 39$	$N = 59$	$N = 199$	Reference
1	5.0300(−3)	5.6651(−3)	5.7845(−3)	5.8722(−3)	5.8809(−3)
2	2.3271(−3)	2.2927(−3)	2.2855(−3)	2.2797(−3)	2.2791(−3)
3	1.3207(−3)	1.3019(−3)	1.2977(−3)	1.2943(−3)	1.2939(−3)
4	8.8058(−4)	8.6826(−4)	8.6542(−4)	8.6306(−4)	8.6280(−4)
5	8.6768(−4)	8.5642(−4)	8.5393(−4)	8.5192(−4)	8.5170(−4)
6	5.0656(−4)	4.9984(−4)	4.9820(−4)	4.9679(−4)	4.9662(−4)
7	4.0501(−4)	3.9970(−4)	3.9837(−4)	3.9720(−4)	3.9706(−4)
8	3.3417(−4)	3.2985(−4)	3.2874(−4)	3.2775(−4)	3.2763(−4)
9	2.8222(−4)	2.7862(−4)	2.7767(−4)	2.7682(−4)	2.7671(−4)
10	2.8495(−4)	2.8138(−4)	2.8047(−4)	2.7966(−4)	2.7956(−4)
11	2.1400(−4)	2.1136(−4)	2.1064(−4)	2.0998(−4)	2.0989(−4)
12	1.8852(−4)	1.8622(−4)	1.8559(−4)	1.8499(−4)	1.8491(−4)
13	1.6796(−4)	1.6594(−4)	1.6537(−4)	1.6483(−4)	1.6476(−4)
14	1.5101(−4)	1.4921(−4)	1.4870(−4)	1.4821(−4)	1.4814(−4)
15	1.3681(−4)	1.3520(−4)	1.3474(−4)	1.3429(−4)	1.3423(−4)
16	1.2475(−4)	1.2331(−4)	1.2289(−4)	1.2247(−4)	1.2242(−4)
17	1.1442(−4)	1.1311(−4)	1.1273(−4)	1.1234(−4)	1.1229(−4)
18	1.0547(−4)	1.0428(−4)	1.0392(−4)	1.0357(−4)	1.0352(−4)
19	9.7655(−5)	9.6571(−5)	9.6241(−5)	9.5906(−5)	9.5859(−5)
20	9.0783(−5)	8.9789(−5)	8.9483(−5)	8.9169(−5)	8.9125(−5)

Table 2
The group transmission factors B_i^* for the five-region, 20-group, downscatter-only problem

i	$N = 19$	$N = 39$	$N = 59$	$N = 199$	Reference
1	1.0453(−2)	1.0453(−2)	1.0453(−2)	1.0453(−2)	1.0453(−2)
2	1.9995(−4)	1.9993(−4)	1.9993(−4)	1.9993(−4)	1.9993(−4)
3	6.9020(−5)	6.9014(−5)	6.9013(−5)	6.9012(−5)	6.9012(−5)
4	3.5398(−5)	3.5394(−5)	3.5393(−5)	3.5393(−5)	3.5393(−5)
5	3.5354(−5)	3.5351(−5)	3.5350(−5)	3.5350(−5)	3.5350(−5)
6	1.4901(−5)	1.4900(−5)	1.4899(−5)	1.4899(−5)	1.4899(−5)
7	1.0718(−5)	1.0716(−5)	1.0716(−5)	1.0716(−5)	1.0716(−5)
8	8.0874(−6)	8.0865(−6)	8.0864(−6)	8.0863(−6)	8.0863(−6)
9	6.3211(−6)	6.3204(−6)	6.3203(−6)	6.3202(−6)	6.3202(−6)
10	6.1280(−6)	6.1273(−6)	6.1272(−6)	6.1271(−6)	6.1271(−6)
11	4.1843(−6)	4.1838(−6)	4.1837(−6)	4.1837(−6)	4.1837(−6)
12	3.4897(−6)	3.4893(−6)	3.4893(−6)	3.4892(−6)	3.4892(−6)
13	2.9549(−6)	2.9545(−6)	2.9545(−6)	2.9545(−6)	2.9545(−6)
14	2.5336(−6)	2.5333(−6)	2.5332(−6)	2.5332(−6)	2.5332(−6)
15	2.1956(−6)	2.1953(−6)	2.1953(−6)	2.1953(−6)	2.1953(−6)
16	1.9203(−6)	1.9200(−6)	1.9200(−6)	1.9200(−5)	1.9200(−5)
17	1.6930(−6)	1.6928(−6)	1.6927(−6)	1.6927(−6)	1.6927(−6)
18	1.5031(−6)	1.5030(−6)	1.5029(−6)	1.5029(−6)	1.5029(−6)
19	1.3430(−6)	1.3428(−6)	1.3428(−6)	1.3428(−6)	1.3428(−6)
20	1.2066(−6)	1.2065(−6)	1.2064(−6)	1.2064(−6)	1.2064(−6)

For a given N, we have confirmed that the numerical results obtained for the albedos, transmission factors and other quantities of interest with the scalar, vector and coupled P_N methods showed, as expected, a level of agreement that was compatible with the machine precision (at least 9 figures of agreement in 16 decimal-digit computations). In addition, as is typical of the P_N method (Garcia and Siewert, 1996; Caldeira et al., 1998a; 1998b), we can see that the transmission factors converge faster than the albedos, as N increases. Finally, in Table 3 we compare the CPU times spent by the scalar ($G_d = 20$, $G_u = 0$), coupled ($G_d = G_u = 10$) and vector ($G_d = 0$, $G_u = 20$) methods to solve this problem on a 400-MHz Pentium II PC, for several orders of the P_N approximation. It can be seen that the coupled method yields substantial savings in computer time over the vector method.

Table 3
CPU times[a] (min.) for solving the five-region, 20-group, downscatter-only problem

N	Scalar ($G_d = 20$)	Coupled ($G_d = 10$)	Vector ($G_d = 0$)
19	0.5	1.2	1.8
29	1.5	2.9	7.0
39	3.5	6.2	12.7
59	10.7	18.6	49.1

[a]Pentium II, 400-MHz clock, 128-MB RAM.

6.2 Calculation of double-differential thermal albedos in 42 groups for a concrete slab

This computationally challenging problem was formulated in a recent work where the F_N method was extended for multigroup transport problems with upscattering (Garcia and Siewert, 1998) and subsequently used by Siewert (2000) to test his discrete-ordinates solution to the same class of problems. It consists of a 100-cm-thick concrete slab irradiated on one side by a normally incident, uniform beam of neutrons in one of the 42 thermal groups that span the energy range from 0 to 4 eV in the WIMS group structure (Kim, 1990). Noting that in this case $G_d = 0$ and $G = G_u = 42$, we are required to solve Eq. (11) with $\mathbf{Q}(z, \mu) = 0$, subject to the boundary conditions given by Eqs. (15a) and (15b) with

$$\mathbf{L}(\mu) = \mathbf{F}\delta(\mu - \mu_0) \tag{63a}$$

and

$$\mathbf{R}(\mu) = \mathbf{0}, \tag{63b}$$

for $\mu \in (0, 1]$. In Eq. (63a), $\mu_0 = 1$ and the vector $\mathbf{F}$ has components $F_i = \delta_{ij}$ for $i = 1, 2, \ldots, 42$, with $1 \leq j \leq 42$ denoting the group of incidence.

The main results of interest for this problem are the double-differential (in energy and angle) thermal albedos

$$\alpha_{ij}(\mu, \mu_0) = \frac{J_i^-(\mu)}{J_j^+(\mu_0)}, \tag{64}$$

for $i = 1, 2, \ldots, 42$ and $\mu \in (0, 1]$, where $J_i^-(\mu) = \mu\Psi_i(0, -\mu)$ and $J_j^+(\mu_0) = \mu_0 F_j$. These quantities are needed for modelling duct wall reflections in three-dimensional duct calculations (Selph, 1973).

To solve this problem, we have adopted a formulation (Siewert, 1993a) based on the uncollided/collided decomposition

$$\mathbf{\Psi}(z, \mu) = \mathbf{\Psi}_0(z, \mu) + \mathbf{\Psi}_*(z, \mu), \tag{65}$$

where the uncollided flux vector $\mathbf{\Psi}_0(z, \mu)$ must solve the problem formulated by Eq. (11) with zero right-hand side and boundary conditions specified by Eqs. (15) and (63), and the collided flux vector $\mathbf{\Psi}_*(z, \mu)$ must solve Eq. (11) with

$$\mathbf{Q}(z, \mu) = \frac{1}{2}\sum_{\ell=0}^{\mathcal{L}} P_\ell(\mu)\mathbf{C}_\ell \int_{-1}^{1} P_\ell(\mu')\mathbf{\Psi}_0(z, \mu')\mathrm{d}\mu' \tag{66}$$

subject to vacuum boundary conditions at z_L and z_R. As the uncollided solution can be readily seen to be

$$\mathbf{\Psi}_0(z,\mu) = \mathrm{e}^{-\mathbf{\Sigma}(z-z_L)/\mu}\mathbf{F}\delta(\mu-\mu_0) \tag{67a}$$

and

$$\mathbf{\Psi}_0(z,-\mu) = \mathbf{0}, \tag{67b}$$

for $\mu \in (0,1]$, we can write Eq. (66) simply as

$$\mathbf{Q}(z,\mu) = \frac{1}{2}\left[\sum_{\ell=0}^{\mathcal{L}} P_\ell(\mu)\mathbf{C}_\ell P_\ell(\mu_0)\right]\mathrm{e}^{-\mathbf{\Sigma}(z-z_L)/\mu_0}\mathbf{F}. \tag{68}$$

Since our solution for the collided problem was found by a mere specialization of the approach discussed in Section 3 for the source defined by Eq. (68), we chose, to save space, not to report here the specific expressions that were obtained for the collided solution.

We list in Table 4 our P_{89} results for the thermal albedos $\alpha_{ij}(\mu,\mu_0)$, $i = 1,2,\ldots,42$ and $j = 4$. These results are in agreement, within ±4 in the last figure shown, with the numerical results reported for the F_N (Garcia and Siewert, 1998) and discrete-ordinates (Siewert, 2000) methods. We should mention that to be able to generate the results reported in Table 4, we had to execute our program in double precision on a long-word machine (CRAY J90). The reason for this requirement is that the cross-section set that defines the problem is such that the matrices $\mathbf{A}$ and $\mathbf{B}$ defined respectively by Eqs. (23) and (27) turn out to be near defective, and, consequently, a destructive loss of precision occurs when their corresponding eigensystems are solved in double-precision on a short-word computer. In passing, we note that we have used for this purpose the sequence of EISPACK subroutines BALANC, ELMHES, ELTRAN, HQR2 and BALBAK (Smith et al., 1976), and have also made an independent implementation using subroutine DGEEV of the LAPACK package (Anderson et al., 1995). We have found that both of these packages perform similarly in terms of accuracy, but LAPACK is more economical, since subroutine DGEEV provides the left and right eigenvectors at once (recall that to compute the $\mathbf{T}^\dagger$-vectors introduced in Section 3 we need the left eigenvectors of $\mathbf{A}$ or $\mathbf{B}$). Thus, to avoid the excessive loss of precision that occurs in the computation of the eigenvalues and eigenvectors for this problem without having to adopt a more complex methodology (singular value decomposition, for example), we have decided to perform the calculation in a much higher precision level (the 32 decimal digits provided by the CRAY J90 computer) than that targeted for the eigenvalues and eigenvectors (9 decimal digits, at least). We note that Siewert (2000) has reported the occurrence of a similar difficulty during his implementation of the discrete-ordinates method for solving this problem.

6.3 One-dimensional model of a fast reactor shield

This shielding problem is defined, as shown in Fig. 2, by seven material regions and an isotropic neutron flux that leaves the reactor core and strikes the left boundary of the system. The energy distribution of the incoming neutrons is taken to be that of fission neutrons and is described by a 21-group representation of the Watt spectrum. In addition, we note that on the right we have a vacuum boundary and that the region dimensions and compositions are given in Table 5.

To define a cross-section set for the problem, we have performed a preliminary calculation with a modified version of the discrete-ordinates ANISN-W code (Soltesz and Disney, 1970), using a nonuniform spatial discretization with a total of 1061 mesh intervals, quadrature order 16 and fine-group cross sections from the VITAMIN-B6 library (White et al., 1994). This library has a group structure with 199 neutron groups in the range 10^{-5} eV–19.64 MeV and 42 groups in the range 1 keV–30 MeV for gammas resulting from (n,γ) reactions, and includes Legendre moments of transfer cross sections of order up to $\mathcal{L} = 7$. The results of the preliminary ANISN-W calculation were subsequently used to collapse the cross sections to a 25-group structure consisting of 21 neutron groups (12 fast and 9 thermal) and four gamma groups (numbered 22 through 25), the upper and lower limits of which are given in Table 6, along with the components L_i, $i = 1,2,\ldots,25$, of the vector $\mathbf{L}$ that defines the incident particle fluxes.

Table 4
P_{89} results for the double-differential thermal albedos $\alpha_{ij}(\mu, \mu_0)$ with $j = 4$ and $\mu_0 = 1$

i	$\mu = 0.1$	$\mu = 0.2$	$\mu = 0.3$	$\mu = 0.4$	$\mu = 0.5$	$\mu = 0.6$	$\mu = 0.7$	$\mu = 0.8$	$\mu = 0.9$	$\mu = 1.0$
1	3.953(−10)	8.996(−10)	1.462(−9)	2.050(−9)	2.642(−9)	3.225(−9)	3.790(−9)	4.332(−9)	4.848(−9)	5.337(−9)
2	1.956(−7)	4.425(−7)	7.023(−7)	9.578(−7)	1.201(−6)	1.426(−6)	1.634(−6)	1.822(−6)	1.991(−6)	2.143(−6)
3	1.197(−4)	2.180(−4)	2.938(−4)	3.489(−4)	3.856(−4)	4.061(−4)	4.124(−4)	4.062(−4)	3.891(−4)	3.624(−4)
4	1.818(−2)	3.096(−2)	3.896(−2)	4.290(−2)	4.339(−2)	4.097(−2)	3.607(−2)	2.904(−2)	2.017(−2)	9.706(−3)
5	9.696(−3)	1.794(−2)	2.463(−2)	2.990(−2)	3.391(−2)	3.680(−2)	3.871(−2)	3.978(−2)	4.009(−2)	3.975(−2)
6	5.335(−3)	1.017(−2)	1.428(−2)	1.762(−2)	2.024(−2)	2.221(−2)	2.358(−2)	2.441(−2)	2.477(−2)	2.470(−2)
7	8.146(−4)	1.530(−3)	2.104(−3)	2.533(−3)	2.824(−3)	2.988(−3)	3.037(−3)	2.984(−3)	2.837(−3)	2.608(−3)
8	7.581(−4)	1.422(−3)	1.951(−3)	2.340(−3)	2.596(−3)	2.729(−3)	2.752(−3)	2.674(−3)	2.506(−3)	2.258(−3)
9	7.373(−4)	1.383(−3)	1.895(−3)	2.268(−3)	2.509(−3)	2.627(−3)	2.634(−3)	2.541(−3)	2.357(−3)	2.091(−3)
10	7.227(−4)	1.358(−3)	1.862(−3)	2.228(−3)	2.462(−3)	2.574(−3)	2.575(−3)	2.474(−3)	2.283(−3)	2.010(−3)
11	6.854(−4)	1.291(−3)	1.773(−3)	2.125(−3)	2.351(−3)	2.460(−3)	2.463(−3)	2.369(−3)	2.188(−3)	1.927(−3)
12	6.542(−4)	1.236(−3)	1.701(−3)	2.042(−3)	2.264(−3)	2.373(−3)	2.379(−3)	2.292(−3)	2.119(−3)	1.871(−3)
13	6.506(−4)	1.232(−3)	1.700(−3)	2.045(−3)	2.272(−3)	2.387(−3)	2.400(−3)	2.319(−3)	2.153(−3)	1.911(−3)
14	5.983(−4)	1.137(−3)	1.575(−3)	1.902(−3)	2.120(−3)	2.237(−3)	2.259(−3)	2.194(−3)	2.052(−3)	1.838(−3)
15	1.086(−3)	2.073(−3)	2.880(−3)	3.490(−3)	3.906(−3)	4.137(−3)	4.197(−3)	4.102(−3)	3.864(−3)	3.496(−3)
16	1.659(−3)	3.195(−3)	4.482(−3)	5.485(−3)	6.203(−3)	6.648(−3)	6.839(−3)	6.796(−3)	6.538(−3)	6.086(−3)
17	1.999(−3)	3.895(−3)	5.525(−3)	6.840(−3)	7.831(−3)	8.510(−3)	8.892(−3)	9.000(−3)	8.856(−3)	8.480(−3)
18	4.808(−3)	9.560(−3)	1.383(−2)	1.747(−2)	2.042(−2)	2.269(−2)	2.431(−2)	2.530(−2)	2.572(−2)	2.561(−2)
19	4.458(−3)	9.102(−3)	1.350(−2)	1.746(−2)	2.092(−2)	2.385(−2)	2.624(−2)	2.812(−2)	2.950(−2)	3.043(−2)
20	4.141(−3)	8.641(−3)	1.308(−2)	1.725(−2)	2.107(−2)	2.447(−2)	2.745(−2)	3.001(−2)	3.215(−2)	3.390(−2)
21	2.351(−3)	4.980(−3)	7.639(−3)	1.021(−2)	1.262(−2)	1.484(−2)	1.684(−2)	1.864(−2)	2.021(−2)	2.158(−2)
22	1.530(−3)	3.267(−3)	5.048(−3)	6.793(−3)	8.454(−3)	1.000(−2)	1.143(−2)	1.273(−2)	1.389(−2)	1.493(−2)
23	1.081(−3)	2.319(−3)	3.601(−3)	4.867(−3)	6.083(−3)	7.229(−3)	8.294(−3)	9.272(−3)	1.016(−2)	1.096(−2)
24	1.140(−3)	2.456(−3)	3.829(−3)	5.196(−3)	6.518(−3)	7.773(−3)	8.950(−3)	1.004(−2)	1.104(−2)	1.195(−2)
25	1.843(−3)	3.994(−3)	6.259(−3)	8.534(−3)	1.076(−2)	1.289(−2)	1.490(−2)	1.679(−2)	1.855(−2)	2.017(−2)
26	2.057(−3)	4.488(−3)	7.081(−3)	9.719(−3)	1.233(−2)	1.486(−2)	1.730(−2)	1.961(−2)	2.178(−2)	2.382(−2)
27	3.281(−3)	7.229(−3)	1.152(−2)	1.596(−2)	2.043(−2)	2.486(−2)	2.919(−2)	3.338(−2)	3.741(−2)	4.126(−2)
28	4.483(−3)	1.001(−2)	1.616(−2)	2.271(−2)	2.947(−2)	3.634(−2)	4.321(−2)	5.003(−2)	5.675(−2)	6.333(−2)
29	7.244(−3)	1.640(−2)	2.690(−2)	3.836(−2)	5.052(−2)	6.318(−2)	7.616(−2)	8.935(−2)	1.026(−1)	1.159(−1)
30	5.715(−3)	1.306(−2)	2.162(−2)	3.113(−2)	4.138(−2)	5.220(−2)	6.347(−2)	7.505(−2)	8.687(−2)	9.884(−2)
31	4.926(−3)	1.131(−2)	1.881(−2)	2.721(−2)	3.633(−2)	4.603(−2)	5.618(−2)	6.669(−2)	7.747(−2)	8.845(−2)
32	4.087(−3)	9.402(−3)	1.567(−2)	2.272(−2)	3.041(−2)	3.861(−2)	4.724(−2)	5.619(−2)	6.540(−2)	7.480(−2)
33	4.123(−3)	9.494(−3)	1.585(−2)	2.300(−2)	3.083(−2)	3.920(−2)	4.802(−2)	5.720(−2)	6.666(−2)	7.633(−2)
34	4.565(−3)	1.052(−2)	1.756(−2)	2.552(−2)	3.424(−2)	4.358(−2)	5.343(−2)	6.371(−2)	7.432(−2)	8.519(−2)
35	4.269(−3)	9.830(−3)	1.642(−2)	2.387(−2)	3.203(−2)	4.080(−2)	5.006(−2)	5.973(−2)	6.973(−2)	8.000(−2)
36	3.143(−3)	7.231(−3)	1.207(−2)	1.755(−2)	2.355(−2)	3.000(−2)	3.683(−2)	4.396(−2)	5.135(−2)	5.894(−2)
37	3.131(−3)	7.193(−3)	1.200(−2)	1.743(−2)	2.339(−2)	2.979(−2)	3.658(−2)	4.367(−2)	5.103(−2)	5.859(−2)
38	3.011(−3)	6.901(−3)	1.149(−2)	1.668(−2)	2.236(−2)	2.848(−2)	3.496(−2)	4.174(−2)	4.878(−2)	5.603(−2)
39	2.748(−3)	6.275(−3)	1.042(−2)	1.510(−2)	2.022(−2)	2.574(−2)	3.158(−2)	3.770(−2)	4.406(−2)	5.062(−2)
40	2.293(−3)	5.203(−3)	8.605(−3)	1.243(−2)	1.661(−2)	2.111(−2)	2.588(−2)	3.088(−2)	3.609(−2)	4.147(−2)
41	1.583(−3)	3.552(−3)	5.828(−3)	8.369(−3)	1.114(−2)	1.412(−2)	1.727(−2)	2.058(−2)	2.403(−2)	2.760(−2)
42	5.923(−4)	1.297(−3)	2.091(−3)	2.965(−3)	3.909(−3)	4.916(−3)	5.982(−3)	7.101(−3)	8.268(−3)	9.480(−3)

We have solved this problem with our coupled P_N method, using the scalar method for the 12 groups of fast neutrons and the vector method for the 9 groups of thermal neutrons and the 4 groups of gammas. Therefore, the group structure has $G_d = 12$ and $G_u = 13$. In Table 7, we report our P_{47} postprocessed results for the group angular fluxes exiting the right boundary of the system along four values of the direction variable μ that

are ordinates in the S_{48} approximation used by the ANISN-W code to generate the results labeled as S_{N+1} in the table. The ANISN-W results are based on the same spatial discretization scheme that was used for the preliminary calculation (1061 intervals). It can be seen that the P_{47} and S_{48} results agree very well, with a maximum relative difference of less than 0.16% between these results.

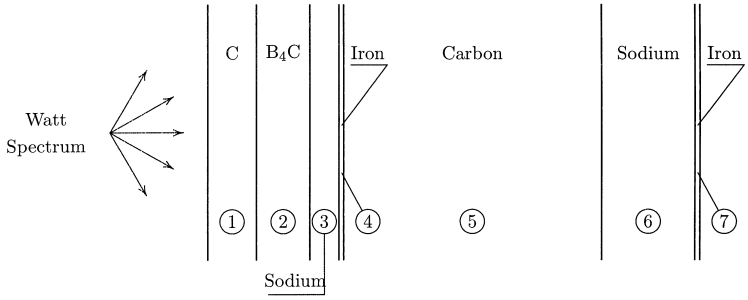

Fig. 2. One-dimensional shield model of the REARA experimental fast reactor

Table 5
Region dimensions (cm) and material densities [atoms/(barn.cm)]

Region #	Component	Dimension	Carbon	Boron-10	Sodium	Iron
1	Reflector	16.85	2.1305(−2)			
2	Removable Shield	17.73	1.5671(−2)	1.2394(−2)		
3	Coolant	34.00			2.2521(−2)	
4	Core Barrel	1.25				5.3231(−2)
5	Shield	67.50	8.0233(−2)			
6	Coolant	30.00			2.2521(−2)	
7	Reactor Tank	5.08				5.3231(−2)

Table 6
Group structure and incident particle fluxes for the shielding problem

i	Upper Energy (eV)	Lower Energy (eV)	L_i	i	Upper Energy (eV)	Lower Energy (eV)	L_i
1	1.9640(+7)	2.3069(+6)	0.0011	14	1.8554(+0)	1.0800(+0)	0.0024
2	2.3069(+6)	1.4227(+6)	0.7264	15	1.0800(+0)	8.0000(−1)	0.0019
3	1.4227(+6)	7.4274(+5)	0.9717	16	8.0000(−1)	5.0000(−1)	0.0016
4	7.4274(+5)	3.3373(+5)	1.0000	17	5.0000(−1)	2.7500(−1)	0.0012
5	3.3373(+5)	1.9255(+5)	0.8421	18	2.7500(−1)	1.2500(−1)	0.0009
6	1.9255(+5)	8.2503(+4)	0.6619	19	1.2500(−1)	4.0000(−2)	0.0006
7	8.2503(+4)	2.4176(+4)	0.4358	20	4.0000(−2)	1.0000(−2)	0.0003
8	2.4176(+4)	3.0354(+3)	0.2259	21	1.0000(−2)	1.0000(−5)	0.0001
9	3.0354(+3)	5.8295(+2)	0.0830	22	3.0000(+7)	5.5000(+6)	0.0
10	5.8295(+2)	4.7851(+1)	0.0347	23	5.5000(+6)	1.3400(+6)	0.0
11	4.7851(+1)	1.7604(+1)	0.0112	24	1.3400(+6)	2.0000(+5)	0.0
12	1.7604(+1)	6.4760(+0)	0.0066	25	2.0000(+5)	1.0000(+3)	0.0
13	6.4760(+0)	1.8554(+0)	0.0036				

Table 7
The group angular fluxes exiting the right boundary of the shield for $N = 47$

	$\mu = 0.0323802$		$\mu = 0.2873625$		$\mu = 0.5772247$		$\mu = 0.9058791$		$\mu = 0.9987710$	
i	P_N	S_{N+1}	P_N	S_{N+1}	P_N	S_{N+1}	P_N	S_{N+1}	P_N	S_{N+1}
1	1.856(−9)	1.856(−9)	3.381(−9)	3.381(−9)	6.184(−9)	6.183(−9)	1.357(−8)	1.356(−8)	1.812(−8)	1.812(−8)
2	2.815(−7)	2.814(−7)	5.100(−7)	5.096(−7)	9.435(−7)	9.429(−7)	2.018(−6)	2.016(−6)	2.745(−6)	2.743(−6)
3	1.227(−6)	1.226(−6)	1.913(−6)	1.912(−6)	2.778(−6)	2.776(−6)	4.208(−6)	4.204(−6)	4.792(−6)	4.788(−6)
4	2.990(−6)	2.987(−6)	4.376(−6)	4.372(−6)	5.642(−6)	5.637(−6)	7.205(−6)	7.199(−6)	7.721(−6)	7.714(−6)
5	2.069(−6)	2.067(−6)	3.114(−6)	3.111(−6)	4.192(−6)	4.189(−6)	5.475(−6)	5.471(−6)	5.880(−6)	5.874(−6)
6	3.396(−6)	3.393(−6)	5.138(−6)	5.133(−6)	7.133(−6)	7.127(−6)	9.465(−6)	9.457(−6)	1.017(−5)	1.016(−5)
7	5.553(−6)	5.549(−6)	8.148(−6)	8.142(−6)	1.057(−5)	1.056(−5)	1.336(−5)	1.335(−5)	1.423(−5)	1.422(−5)
8	8.004(−6)	7.994(−6)	1.181(−5)	1.180(−5)	1.567(−5)	1.565(−5)	2.057(−5)	2.054(−5)	2.218(−5)	2.216(−5)
9	1.059(−5)	1.058(−5)	1.579(−5)	1.577(−5)	2.180(−5)	2.177(−5)	2.974(−5)	2.970(−5)	3.223(−5)	3.219(−5)
10	5.560(−5)	5.555(−5)	8.246(−5)	8.239(−5)	1.107(−4)	1.106(−4)	1.438(−4)	1.437(−4)	1.537(−4)	1.536(−4)
11	2.770(−5)	2.768(−5)	4.106(−5)	4.103(−5)	5.501(−5)	5.496(−5)	7.114(−5)	7.108(−5)	7.589(−5)	7.583(−5)
12	3.037(−5)	3.036(−5)	4.506(−5)	4.504(−5)	6.050(−5)	6.047(−5)	7.860(−5)	7.856(−5)	8.399(−5)	8.395(−5)
13	4.126(−5)	4.124(−5)	6.123(−5)	6.120(−5)	8.249(−5)	8.245(−5)	1.081(−4)	1.081(−4)	1.159(−4)	1.158(−4)
14	1.795(−5)	1.794(−5)	2.664(−5)	2.663(−5)	3.601(−5)	3.599(−5)	4.756(−5)	4.754(−5)	5.113(−5)	5.111(−5)
15	9.297(−6)	9.293(−6)	1.380(−5)	1.380(−5)	1.875(−5)	1.874(−5)	2.504(−5)	2.503(−5)	2.703(−5)	2.702(−5)
16	1.377(−5)	1.376(−5)	2.047(−5)	2.046(−5)	2.795(−5)	2.794(−5)	3.773(−5)	3.771(−5)	4.089(−5)	4.087(−5)
17	2.301(−5)	2.300(−5)	3.428(−5)	3.426(−5)	4.729(−5)	4.727(−5)	6.515(−5)	6.512(−5)	7.114(−5)	7.112(−5)
18	1.007(−4)	1.007(−4)	1.508(−4)	1.508(−4)	2.150(−4)	2.149(−4)	3.175(−4)	3.173(−4)	3.553(−4)	3.552(−4)
19	4.159(−4)	4.156(−4)	6.243(−4)	6.239(−4)	9.080(−4)	9.074(−4)	1.418(−3)	1.417(−3)	1.621(−3)	1.620(−3)
20	1.780(−4)	1.779(−4)	2.655(−4)	2.653(−4)	3.871(−4)	3.867(−4)	6.259(−4)	6.254(−4)	7.290(−4)	7.283(−4)
21	9.149(−6)	9.138(−6)	1.316(−5)	1.315(−5)	1.841(−5)	1.838(−5)	2.899(−5)	2.894(−5)	3.396(−5)	3.391(−5)
22	6.015(−4)	6.011(−4)	1.951(−3)	1.951(−3)	2.507(−3)	2.507(−3)	2.665(−3)	2.665(−3)	2.712(−3)	2.712(−3)
23	1.035(−3)	1.035(−3)	3.281(−3)	3.280(−3)	6.119(−3)	6.119(−3)	7.441(−3)	7.441(−3)	7.634(−3)	7.634(−3)
24	3.644(−3)	3.644(−3)	5.458(−3)	5.458(−3)	7.666(−3)	7.666(−3)	1.035(−2)	1.035(−2)	1.106(−2)	1.106(−2)
25	6.219(−4)	6.217(−4)	7.691(−4)	7.689(−4)	8.769(−4)	8.766(−4)	1.006(−3)	1.006(−3)	1.056(−3)	1.055(−3)

In Table 8, we show, for several values of N, the execution (CPU) times for running this problem on a 350-MHz Pentium II PC and the maximum percent deviations observed in the total fluxes and currents with respect to the P_{63} results. First of all, we note that the S_{64} calculation of ANISN-W did not converge for reasons unknown to us, and this is why the S_{N+1} columns in Table 8 do not carry the corresponding $N = 63$ entries. In addition, we have found, for this and other problems that we solved, that the P_N method is more economical than the S_{N+1} method in low order but, after a certain value of N (near 31 in this case), it becomes more time consuming. We believe that this observation can be explained by noting that a substantial portion of the computer time in the P_N method is spent computing eigenvalues and eigenvectors and solving full linear systems with Gaussian elimination, which are essentially N^3 processes (with the exception of the eigenvalue calculation in the scalar method which is a N^2 process), while the computer time in the S_{N+1} method should, in principle, grow with N somewhere between N and N^2. Indeed, for this test problem, we have concluded from the times displayed in Table 8 that the ratio between the increase in computer time for, say, approximation $N = N_2$ to that for approximation $N = N_1$ (both with respect to the time spent by approximation $N = 7$) follows a pattern roughly $\propto (N_2/N_1)^{2.73}$ for the P_N method, while in the worst case of the S_{N+1} method ($N_2 = 47$ and $N_1 = 15$) this ratio turns out to be $\approx (47/15)^{1.67}$.

Table 8
CPU times[a] and maximum percent deviations for the shielding problem

	P_N		S_{N+1}	
N	Time (s)	Max. Dev. (%)	Time (s)	Max. Dev. (%)
7	34.8	65.9	554.9	69.9
15	158.6	23.2	652.8	47.4
31	960.0	3.9	820.8	4.6
47	2739.7	1.2	1215.0	1.3
63	6338.2	—	—	—

[a]Pentium II, 350-MHz clock, 512-MB RAM.

7. Concluding remarks

We have reported in this paper a new version of the spatially continuous P_N method for solving multigroup transport problems in plane geometry that is based on a coupling of previously reported scalar and vector P_N methods. From the solutions for the first and third test problems analyzed in this work, we were able to confirm in practice the notion (Caldeira et al., 1998a) that the use of the scalar method in place of the vector method when dealing with the slowing-down part of the calculation yields a substantial reduction in computer time requirements. Still from the point of view of computer time, in order to make the method competitive in high order with methods based on spatial discretizations of the transport equation, we believe that an additional effort should be directed to devising and implementing more economical ways for computing the eigenvalues and eigenvectors for the vector version of the method (perhaps by making use of the banded structure of the eigensystems) and for solving the linear systems that result from the application of the boundary conditions.

Acknowledgements

One of the authors (A.F.D.) whishes to express his gratitude to the *Ministério da Ciência e Tecnologia* for the financial support received from the RHAE program in the course of his doctoral studies. Thanks are also due to L. H. Claro, head of the Nuclear Energy Division, A. Passaro, coordinator of the ENU/EFA Virtual Engineering Laboratory, and A. C. C. Migliano, coordinator of the EFA-E Electromagnetic Systems Laboratory, all of CTA/IEAv, for computer facilities that were used to generate the numerical results reported in this paper, and to the *Núcleo de Atendimento em Computação de Alto Desempenho* at COPPE/UFRJ for the time alloted on the CRAY J90 computer. The work of R.D.M.G. was supported in part by CNPq.

References

Anderson, E., Bai, Z., Bischof, C., Demmel, J., Dongarra J., Du Croz, J., Greenbaum, A., Hammarling, S., McKenney, A., Ostrouchov, S., Sorensen, D. 1995. *LAPACK Users' Guide*, 2nd ed. SIAM, Philadelphia, Pa.

Caldeira, A. D., Dias, A. F., Garcia, R. D. M. 1998a. A P_N solution to the multigroup slowing-down problem—I: basic formulation. *Nucl. Sci. Eng.* **130**, 60–69.

Caldeira, A. D., Dias, A. F., Garcia, R. D. M. 1998b. A P_N solution to the multigroup slowing-down problem—II: the degenerate case. *Nucl. Sci. Eng.* **130**, 70–78.

Dave, J. V., Armstrong, B. H. 1974. Smoothing of the intensity curve obtained from a solution of the spherical harmonics approximation to the transfer equation. *J. Atmos. Sci.* **31**, 1934–1937.

Davison, B. 1957. *Neutron Transport Theory.* Oxford University Press, London.

Dias, A. F. 1999. *The P_N Method for Shielding Calculations in Multislab Geometry* (in Portuguese). Sc. D. thesis, Instituto de Pesquisas Energéticas e Nucleares, São Paulo.

Dias, A. F., Ono, S. 1995. *Conception of the Experimental Reactor Shields* (in Portuguese). Technical Note IEAv-005/95, Centro Técnico Aeroespacial, Instituto de Estudos Avançados, São José dos Campos, SP, Brazil.

Garcia, R. D. M. 2000. An analysis of the source-function integration technique for postprocessing P_N angular fluxes. *Ann. Nucl. Energy* **27**, 1217–1226.

Garcia, R. D. M., Siewert, C. E. 1983. Multislab multigroup transport theory with Lth order anisotropic scattering. *J. Comput. Phys.* **50**, 181–192.

Garcia, R. D. M., Siewert, C. E. 1996. A stable shifted-Legendre projection scheme for generating P_N boundary conditions. *Ann. Nucl. Energy* **23**, 321–332.

Garcia, R. D. M., Siewert, C. E. 1998. The F_N method for multigroup transport theory with upscattering. *Nucl. Sci. Eng.* **130**, 194–212.

Gelbard, E. M. 1968. Spherical harmonics methods: P_L and double-P_L approximations. In: Greenspan, H., Kelber, C. N., Okrent, D. (Eds.), *Computing Methods in Reactor Physics.* Gordon & Breach, New York, pp. 267–358.

Karp, A. H. 1981. Computing the angular dependence of the radiation of a planetary atmosphere. *J. Quant. Spectrosc. Radiat. Transfer* **25**, 403–412.

Kim, J.-D. 1990. *WIMKAL-88, the 1988 Version of the WIMS-KAERI Library.* Report IAEA-NDS-98, IAEA Nuclear Data Section, Vienna.

Kourganoff, V. 1952. *Basic Methods in Transfer Problems.* Clarendon Press, Oxford.

Lee, C. E., Fan, W. C. P., Dias, M. P. 1985. Analytical solutions to the moment transport equations—II: multiregion, multigroup 1-D slab, cylinder, and sphere criticality and source problems. *Ann. Nucl. Energy* **12**, 613–632.

Selph, W. E. 1973. Albedos, ducts, and voids. In: Schaeffer, N. M. (Ed.), *Reactor Shielding for Nuclear Engineers.* U. S. Atomic Energy Comission Office of Information Services, pp. 313–418.

Siewert, C. E. 1993a. A spherical-harmonics method for multi-group or non-gray radiation transport. *J. Quant. Spectrosc. Radiat. Transfer* **49**, 95–106.

Siewert, C. E. 1993b. On intensity calculations in radiative transfer. *J. Quant. Spectrosc. Radiat. Transfer* **50**, 555–560.

Siewert, C. E. 2000. A discrete-ordinates solution for multigroup transport theory with upscattering. *J. Quant. Spectrosc. Radiat. Transfer* **64**, 255-271.

Siewert, C. E., Thomas Jr., J. R. 1987. A method for computing the discrete spectrum basic to multi-group transport theory. *J. Quant. Spectrosc. Radiat. Transfer* **37**, 111–115.

Smith, B. T., Boyle, J. M., Dongarra, J. J., Garbow, B. S., Ikebe, Y., Klema, V. C., Moler, C. B. 1976. *Matrix Eigensystem Routines - EISPACK Guide.* Springer-Verlag, Berlin.

Soltelz, R. G., Disney, R. K. 1970. *Nuclear Rocket Shielding Methods, Modification, Updating, and Input Data Preparation, Volume 4 - One-Dimensional, Discrete Ordinates Transport Technique.* Report WANL-PR-(LL)-034, Westinghouse Astronuclear Laboratory, Pittsburgh, Pa.

White, J. E., Wright, R. Q., Ingersoll, D. T., Roussin, R. W., Greene, N. M., MacFarlane, R. E. 1994. VITAMIN-B6: a fine-group cross section library based on ENDF/B-VI for radiation transport applications. *Proceedings of the International Conference on Nuclear Data for Science and Technology*, May 9–13, 1994. Gatlinburg, Tenn., Vol. 2, pp. 733–736.